Polymer Chemistry

ROYAL SOCIETY OF CHEMISTRY

PAPER

View Article Online
View Journal | View Issue

Cite this: *Polym. Chem.*, 2022, **13**, 2907

Functional nanoporous materials from boronate-containing stimuli-responsive diblock copolymers†

Erigene Bakangura, [a] David Fournier,[b] Fanny Coumes, ‡[b] Patrice Woisel, [b] Daniel Grande [a] and Benjamin Le Droumaguet *[a]

Received 21st February 2022,
Accepted 11th April 2022

DOI: 10.1039/d2py00237j

rsc.li/polymers

Functional nanoporous polymeric materials have been prepared from novel polystyrene-*block*-poly(ethylene oxide) (PS-*b*-PEO) diblock copolymer precursors containing a reversible boronate ester junction between both blocks. To this purpose, homopolymers presenting either a boronic acid or a (nitro)catechol end functionality were synthesized. The coupling of each homopolymer presenting complementary chemical functions was successfully achieved under mild conditions and allowed for the generation of the corresponding boronate ester-containing diblock copolymers. Upon orientation of these precursors on silicon wafers *via* solvent vapor annealing, the resulting films were submitted to PEO etching through selective cleavage of the boronate ester junction under mild acidic conditions. SEM micrographs of the as-obtained thin films revealed the generation of 12 nm-diameter oriented cylindrical nanopores perpendicular to the silicon support surface.

Introduction

Diblock copolymers can self-assemble into well-organized microphase-separated morphologies in bulk, namely body-centered spheres, alternating lamellae, bicontinuous gyroids or hexagonally close-packed cylinders.[1–3] For a given AB diblock copolymer, the structure and size of A and B domains are governed directly by the product of degree of polymerization and Flory Huggins interaction parameter ($N\chi_{AB}$), and volume fraction of each block ($f_{A\&B}$).[2] Nanoporous materials with controlled morphology can be produced from hexagonally close-packed cylinders or bicontinuous gyroids upon removal of the sacrificial minority block.[4,5] The sacrificial polymer block is readily removed either by chemical etching[6–13] or by selective cleavage of the functional junction positioned between both blocks.[14–18] The latter strategy is much more attractive because it presents some inherent advantages: (i) it can be achieved in environmentally benign experimental conditions, (ii) it is independent of the chemical nature of the polymer segments, but more importantly (iii) it can release a reactive functional group at the pore surface meant for further chemical reaction or functionalization.

Nanoporous materials featuring reactive surfaces are of particular interest due to their potential application in nanolithography, supported catalysis, nano-templating, sensor design and membrane-based separation. A large variety of cleavable junctions has been implemented to generate functional nanopores, including trityl ether,[14,15] acetal,[19,20] and *o*-nitrobenzyl ester[21–25] functions. Acid-cleavable connections, such as trityl ether or acetal moieties, have hitherto been reported to release low reactive tertiary alcohols. *O*-Nitrobenzyl (ONB) derivatives in the form of esters, carbamates, and carbonates can readily break under UV irradiation to release carboxylic acid, amine or alcohol functions, respectively.[26] Although most junctions can be cleaved under mild experimental conditions, the reactivity of released functional groups is limited under certain reaction conditions, making post-modification difficult.

The utilization of a reversible junction has been introduced as a convenient pathway for controlling the pore surface chemistry. A straightforward approach uses reversible non-covalent junctions such as van der Waals, hydrogen bonding, ionic, or coordinative interactions.[18,27] However, the functional groups accessible through non-covalent interactions are limited. Alternatively, reversible covalent linkers including disulfide,[28,29] oxyimines[30] and Diels–Alder derivatives[31] have been incorporated into block copolymers to generate nanoporous films. A reversible covalent disulfide bond was demonstrated to decorate nanopores with thiol functional groups after its scission by a redox solution. The thiol–gold interactions were exploited to evidence the availability of thiol func-

[a]*Univ Paris Est Creteil, CNRS, ICMPE, UMR 7182, 2 Rue Henri Dunant, F-94320 Thiais, France. E-mail: ledroumaguet@icmpe.cnrs.fr*
[b]*Univ. Lille, CNRS, INRAE, Centrale Lille, UMR 8207 – UMET – Unité Matériaux et Transformations, F-59000 Lille, France*

†Electronic supplementary information (ESI) available. See DOI: **https://doi.org/10.1039/d2py00237j**

‡Current address: Sorbonne Univ., CNRS, UMR 8232 – IPCM – Institut Parisien de Chimie Moléculaire – Chimie des Polymères (CDP) team, 75252 Paris Cedex 05, France.

tional groups inside the nanopores.[28] Afterward, Khan and coworkers[30] reported on the synthesis of a dynamic covalent copolymer (PS-*b*-PEO) using an oxyimine derivative. The scission of oxyimine resulted in oxy-amine-functionalized nanopores upon selective removal of the PEO phase in the corresponding as-prepared thin film.

The integration of a cleavable linker into block copolymers has been performed through different synthetic methods. A commonly employed approach consists in polymerizing monomers using a macroinitiator containing a cleavable linker.[17,24,32,33] This macroinitiator-based route relies on synthesizing a first polymer block with a functional group that can be employed to initiate the second chain polymerization (*i.e.* controlled free-radical, anionic, or cationic polymerizations) to grow a second polymer block. A disulfide-linked PS-SS-PEO diblock copolymer was synthesized in this way *via* reversible-addition fragmentation chain transfer (RAFT) polymerization of styrene using a PEO-based macroinitiator containing a disulfide bond, for instance.[28] More recently, a disulfide linkage was conveniently introduced in PS-*b*-PLA diblock copolymer *via* ring-opening polymerization (ROP) of D, L-lactide (LA) using a polystyrene macroinitiator (PS-OH) containing a disulfide bond.[29] Although macroinitiator route leads to the formation of well-defined BCPs, the precise control of the chain size distribution of the second block remains a challenge. In this regard, coupling two preformed end-functionalized homopolymers is a simple alternative approach for the preparation of well-defined block copolymers.[34,35] This strategy allows for the control over polymer chain size distribution while retaining information of individual blocks. Different copolymers have been synthesized through highly efficient "click" chemistry such as copper(I)-catalyzed azide–alkyne cycloaddition (CuAAC),[34] thiol–ene addition[35] or *via* dynamic covalent chemistry such as retro-Diels–Alder or boronic acid reactions. The dynamically reversible condensation of boronic acid with organic diols is more attractive, as the bond reversibility occurs under mild conditions without the use of catalysts. This reaction leads to the formation of a covalent boronate ester group that can be readily cleaved by a slight change in pH or a simple exchange with a competitive group under neutral conditions. This feature is of particular interest in molecular recognition-based applications. Recently, the coupling reaction between boronic acid and nitrocatechol end-functionalized homopolymers was employed to synthesize a variety of block copolymers featuring a multistimuli-responsive reversible covalent boronate ester junction.[36,37] The reaction occured under neutral conditions upon removal of water as a byproduct to facilitate the boronate ester bond formation. The reversibility of the coupling reaction and responsiveness of boronate ester formed from nitrocatechol were demonstrated for such copolymer-based nanoparticles in aqueous suspension upon applying various stimuli, such as pH change, addition of sugar, and UV irradiation.[36]

Herein, we describe a novel approach for producing nanoporous materials utilizing a dynamic boronate ester as a labile reversible junction sensitive to different stimuli, such as physiological pH, UV irradiation, and interactions with carbohydrates. Catechol- or boronic acid-terminated polystyrenes are synthesized *via* the Reversible Addition–Fragmentation chain Transfer (RAFT) polymerization process. A series of new polystyrene-*block*-poly(ethylene oxide) (PS-*b*-PEO) block copolymers containing a boronate ester junction are prepared by coupling boronic acid-appended PEO and catechol-terminated PS samples. The diblock copolymers can self-assemble into well-defined morphologies in thin films through spin coating, followed by controlled solvent vapor annealing. The functional nanoporous polymers are then obtained through the removal of the PEO segment by immersing the as-obtained thin films in a slightly acidic ethanol solution, thus releasing reactive catechols or boronic acid functions at the pore surface. The as-prepared nanoporous materials can potentially be utilized as supports for biomaterial immobilization, protein separation or heterogeneous catalysis.

Materials & methods

Materials

Poly(ethylene oxide) methyl ether (MeO-PEO-OH, M_n (^{1}H NMR) = 5280 g mol^{-1}, M_n (SEC) = 5049 g mol^{-1}, $Đ$ = 1.05), triethylamine (TEA, ≥99.5%), 4-dimethylaminopyridine (DMAP, ≥99%), *N*,*N*′-dicyclohexylcarbodiimide (DCC, 99%), 1,8-diazabicycloundec-7-ene (DBU, 98%), succinic anhydride (SAH, ≥99%), *N*-hydroxysuccinimide (NHS, 98%), dopamine hydrochloride (98%), 3-((bromomethyl)phenyl)boronic acid (3BrPBA, 90%) and 2-(dodecylthiocarbonothioylthio)-2-methylpropanoic acid (DDMAT, 98%) were purchased from Sigma Aldrich and used as received without further purification. Styrene (≥99%) was obtained from Sigma Aldrich and flushed through a column of neutral alumina prior to use. Nitrodopamine (ND) and 2-(1-isobutyl)sulfanylthiocarbonylsulfanyl-2-methylpropionic acid and boronic acid-terminated chain transfer agent (Bora-CTA) were synthesized according to already reported procedures.[36] Azobis(isobutyronitrile) (AIBN) was recrystallized from methanol, dried under vacuum and stored in small individual vials at 4 °C prior to use for safety reasons.

Synthesis of carboxylic acid end-functionalized poly(ethylene oxide) (MeO-PEO-COOH)

Poly(ethylene oxide) methyl ether (MeO-PEO) was converted to carboxylic acid-terminated poly (ethylene oxide) methyl ether (MeO-PEO-COOH) by esterification with succinic anhydride. In a 250 mL round-bottom flask, dried MeO-PEO (10 g, 2 mmol) was dissolved in 1,4-dioxane (50 mL) at 50 °C and then cooled to 5–10 °C in an ice/water bath. SAH (1 g, 10 mmol), and DMAP (1.22 g, 6 mmol) were added to the solution. The flask was sealed with a rubber septum, evacuated, and filled with nitrogen gas. Triethylamine (TEA, 1.2 g, 12 mmol) was added dropwise to the mixture while stirring. The mixture was allowed to be stirred at RT under a nitrogen atmosphere for

24 h. 1,4-dioxane was removed under vacuum and the residue was dissolved in a 1 M HCl aqueous solution and extracted with chloroform. After washing the organic phase with deionized water, chloroform was removed under reduced pressure. The residue was dissolved in deionized water and dialyzed for 24 h using RC tubing membrane (MWCO of 3.5 kDa). The solution was then acidified with 1 M HCl, extracted with chloroform, dried over $MgSO_4$, filtered off, concentrated under reduced pressure and precipitated in a large volume (20 to 1) of cold diethyl ether. The precipitate was harvested and dried under vacuum to afford the product as a white powder (8.7 g, yield = 85%). The chemical structure of the carboxylic acid-terminated MeO-PEO was confirmed by ^{1}H NMR (400 MHz, DMSO-d_6): δ (ppm): 4.12 (s, 2H, –O–CH_2–CH_2–O–CO–), 3.69 (s, 2H, –O–CH_2–CH_2–O–CO–), 3.51 (s, 446H, –CH_2–CH_2–O– repeating unit), 3.25 (s, 3H, –CH_3), 2.47 (s, 4H, –O–CH_2–CH_2–COOH) (Fig. S1, ESI†).

Synthesis of nitrodopamine (ND)

Nitrodopamine (ND) was obtained following the synthetic procedure reported elsewhere[38] and described as follows. In a 250 mL beaker, dopamine hydrochloride (3.8 g, 20 mmol) and sodium nitrite (3.08 g, 44 mmol) were dissolved in water (50 mL) and cooled to 0–3 °C. Subsequently, sulphuric acid aqueous solution (34.84 mmol in 20 mL of water) was dropwise added to the mixture, and a yellow precipitate was formed. After stirring at room temperature overnight, the precipitate was filtered off and recrystallized from water. After drying the precipitate under the vacuum line, the hemisulfate salt was obtained as dark yellow crystals (3.57 g, yield = 72%). ^{1}H NMR (400 MHz, D_2O): δ (ppm): 7.71 (s, 1H), 6.92 (s, 1H), 3.40–3.29 (m, 2H), 3.22 (t, J = 7.7 Hz, 2H). ^{13}C NMR (101 MHz, DMSO-d_6) δ 154.93, 145.39, 138.12, 127.18, 118.85, 112.29, 39.54, 31.60. The proton and carbon resonance are assigned to the title product using ^{13}C DEPT and 2D ^{1}H, ^{13}C-HSQC (Fig. S2–S5, ESI†).

Synthesis of nitrocatechol end-functionalized poly(ethylene oxide) (MeO-PEO-NC)

In a 100 mL round-bottom flask, dried carboxylated MeO-PEO (MeO-PEO-COOH, 3.5 g, 0.7 mmol) was dissolved in 15 mL of dichloromethane (DCM). *N*-Hydroxysuccinimide (NHS, 0.242 g, 2.1 mmol), and *N*,*N*′-dicyclohexylcarbodiimide (DCC, 0.505 g, 2.45 mmol) were added to the MeO-PEO-COOH solution under positive nitrogen atmosphere. The mixture was allowed to be strirred at room temperature for 24 h, then filtered to remove the dicyclohexylurea by-product, concentrated under reduced pressure and the activated ester was finally precipitated in diethyl ether. The obtained MeO-PEO-NHS (3.3 g, 1 equiv.) was dried under the vacuum line for 6 h, immediately charged in a two-neck round bottom flask, dissolved in 10 mL dry DMF under nitrogen atmosphere. Nitrodopamine hemisulfate (1.03 g, 6 equiv.) was dissolved in 5 mL dry DMF and bubbled with nitrogen gas for 30 min. Nitrodopamine solution was then transferred to the MeO-PEO-NHS solution *via* a canula under N_2 gas. The mixture was stirred at RT for 36 h. 30 mL of deionized water was added to the mixture, and the polymer solution dialyzed for 24 h using a dialysis tubing membrane (RC, MWCO of 3.5 kDa) and the product was extracted three times with dichloromethane. The pure MeO-PEO-NC (2.36 g, 87% yield) was obtained by concentrating the solution under reduced pressure, precipitation in cold diethyl ether, filtration and drying under vacuum. ^{1}H NMR (400 MHz, DMSO-d_6): δ (ppm): 8.00 (s, 1H), 7.48 (s, 1H), 6.67 (s, 1H), 4.11 (s, 2H), 3.69 (s, 2H), 3.51 (s, 463H), 3.36–3.30 (m, 4H), 3.25 (s, 3H), 2.89 (d, J = 7.0 Hz, 2H), 2.33 (d, J = 5.8 Hz, 2H) (Fig. S6, ESI†).

Synthesis of boronic acid end-functionalized poly(ethylene oxide) (MeO-PEO-Bora)

In a two-neck round-bottom flask, carboxylic acid-terminated MeO-PEO-COOH (3.5 g, 0.68 mmol) was dissolved in 10 mL dry DMSO (on 4 Å molecular sieves) over 1,8-diazabicycloundec-7-ene (DBU, 0.156 g, 1.03 mmol) was added to the above solution and the mixture was bubbled with nitrogen gas for 5 min. 3-((bromomethyl)phenyl)boronic acid (3BrPBA) (0.221 g, 1.03 mmol) in 5 mL of dry DMSO was added dropwise to the above mixture for 5 min at RT. The temperature was gradually raised at 70 °C and the reaction medium was allowed to react overnight under nitrogen atmosphere. After cooling the reaction media at RT, the product was precipitated in cold diethyl ether, redissolved in chloroform, washed with 1 N HCl, brine and deionized water. The organic phase was dried over anhydrous $MgSO_4$, filtered, concentrated under reduced pressure, and precipitated in cold diethyl ether. The obtained product was dried under vacuum to give the pure product (73% yield). ^{1}H NMR (400 MHz, DMSO-d_6): δ (ppm): 8.10 (s, 1H), 7.76 (s, 1H), 7.36 (dt, 2H), 5.09 (s, 2H), 4.12 (s, 2H), 3.51 (s, 569H), 3.25 (s, 3H), 2.62 (s, 4H) (Fig. S7, ESI†).

Synthesis of nitrocatechol-functionalized CTA (DDMAT-NC)

In a round-bottom flask equipped with a dropping funnel, 2-(dodecylthiocarbonothioylthio)-2-methylpropanoic acid (DDMAT, 0. 5 g, 1.3 mmol) and *N*,*N*′-dicyclohexylcarbodiimide (DCC, 0.31 g, 1.5 mmol) were dissolved in 15 mL dichloromethane. *N*-Hydroxysuccinimide (NHS, 0.173 g, 1.5 mmol) in dry dichloromethane (5 mL) was dropwise added to this solution. The reaction mixture was stirred at RT for 24 h under nitrogen atmosphere. 30 mL dichloromethane were added to the flask and the organic phase was subsequently washed with saturated sodium hydrogen carbonate solution, deionized water, brine, and finally dried over magnesium sulfate. DDMAT-NHS compound was obtained after filtration and drying under the vacuum line. In a 100 mL round-bottom flask placed in an ice/water bath, DDMAT-NHS (0.515 g, 0.95 mmol) and nitrodopamine (0.205 g, 1.03 mmol) were dissolved in 15 mL dry DMF under nitrogen. Triethylamine (0.105 g, 1.03 mmol) was added, and the yellow solution was stirred at RT for 60 h. The reaction mixture was diluted with 50 mL of a 0.1 M HCl solution, extracted three times with 150 mL diethyl ether. The organic phase was washed twice with deionized water, once with brine and dried over magnesium sulfate. The organic phase was then filtered off, the solvent was removed under reduced pressure to obtain the crude product as a dark

yellow oil. The crude was further purified by flash column chromatography (hexane/DCM: 15/1 (v/v)) to yield the pure product as a yellow crystalline solid (yield = 71%). ^{1}H NMR (400 MHz, DMSO-d_6) δ (ppm): 10.09 (s, 2H), 8.01 (s, 1H), 7.47 (s, 1H), 6.67 (s, 1H), 3.27 (t, 4H), 2.89 (t, 2H), 1.56 (s, 8H), 1.20 (s, 18H), 0.84 (t, 3H). ^{13}C NMR (101 MHz, DMSO-d_6) δ 221.70, 171.17, 151.67, 144.33, 139.85, 128.45, 118.79, 112.62, 57.82, 36.60, 33.79, 32.92, 31.74, 29.31 (q), 28.90, 28.61, 27.86, 25.91, 24.90, 22.55, 14.40. The proton and carbon resonance are assigned to the targeted product using 2D ^{1}H COSY and 2D ^{1}H, ^{13}C HSQC NMR (Fig. S8–S11, ESI†).

Preparation of nitrocatechol end-functionalized polystyrene (PS-NC) *via* RAFT polymerization

Styrene (4.53 g, 43.6 mmol, 400 equiv.), DDMAT-NC (59.4 mg, 0.109 mmol, 1 equiv.), and AIBN (3.57 mg, 0.0218 mmol, 0.22 equiv.) in 1 mL of 1,4-dioxane were mixed in a Schlenk tube and degassed by 3 freeze–pump–thaw cycles. The tube was filled with argon gas, sealed, and placed in an oil bath at 80 °C. Samples were periodically withdrawn *via* a syringe to determine the monomer conversion at different reaction times by ^{1}H NMR spectroscopy. After 60 h, the polymerization was quenched at liquid nitrogen temperature. The polymer was purified by two successive precipitations in a large amount of MeOH and then dried under reduced pressure. SEC was used to determine molecular weight and polydispersity index, respectively. ^{1}H NMR: conversion = 39%. SEC-RI (THF, 1 mL min^{-1}): M_n = 18.3 kg mol^{-1}, $Đ$ = 1.15.

Preparation of boronic acid end-functionalized polystyrene (PS-Bora) *via* RAFT polymerization

Styrene (2.08 g, 20 mmol, 400 equiv.), Bora-CTA (19.3 mg, 0.05 mmol, 1 equiv.), AIBN (1.64 mg, 0.01 mmol, 0.2 equiv.) and 1 mL of 1,4-dioxane were placed in a Schlenk tube and the resulting solution degassed by 3 freeze–pump–thaw cycles. The tube was filled with argon gas, sealed with a rubber septum and placed in an oil bath at 80 °C. After 48 h, the polymerization was quenched at liquid nitrogen temperature. The polymer was purified by successive precipitations (at least twice) in a large volume of MeOH and then dried under reduced pressure. ^{1}H NMR confirmed the purity of the as-obtained polymer and allow for the determination of the monomer conversion by dosage of the chain end functionalities. Experimentally, a sample was withdrawn from the polymerization feed and diluted in $CDCl_3$ prior to ^{1}H NMR comparison of proton signal of monomer and corresponding polymer. SEC was used to determine molecular weight and polydispersity index. ^{1}H NMR: conversion = 52% after 48 h reaction. SEC-RI (THF, 1 mL min^{-1}): $M_{n\ RMN}$ = 21.3 kg mol^{-1}, $Đ$ = 1.08.

Preparation of poly(styrene)-*block*-poly(ethylene oxide) (PS-*b*-PEO)

The poly(styrene)-*block*-poly(ethylene oxide) (PS-*b*-PEO) diblock copolymers, possessing a boronate ester junction were prepared by coupling reaction between homopolymers containing catechol and boronic acid termini. As depicted in Scheme 1, catechol end-functionalized poly(styrene) PS_{167}-Catechol (PS_{167}-NC, 100 mg, 1 equiv.) was dissolved in 35 mL $CHCl_3$ dried over molecular sieves and introduced in a two-necked round bottom flask equipped with a Dean Stark apparatus and a stirring bar. The solution was purged with argon gas for 10 min. Boronic acid end-functionalized methoxypoly(ethylene oxide) (MeO-PEO_{114}-Bora (89.65 mg, 3 equiv.) dissolved in a $CHCl_3$/MeOH: 15/1 (v/v) mL mixture was added dropwise under reflux to the above reaction mixture equipped with drying agent (*e.g.*, molecular sieves 3 Å). The reaction mixture was filtered, concentrated under reduced pressure, and precipitated in cold hexane to remove non reacted polystyrene. The boronate ester containing diblock copolymer was recovered by filtration and dried under vacuum. The as-obtained polymer was then dissolved in dry toluene, cooled at 8 °C and filtered to remove unreacted PEO. The polymer solution was concentrated and precipitated in cold diethyl ether to obtain the PS_{167}-*b*-PEO_{114} diblock copolymer ($M_{n\ SEC,\ THF}$ = 23.6 kg mol^{-1}, $Đ$ = 1.24). ^{1}H NMR was used to confirm the copolymer composition and to determine the volume fraction of each block.

Following the above-mentioned procedure, boronic acid functionalized poly(styrene) (PS_{190}-Bora, 1 equiv.) was coupled with nitrocatechol end-functionalized poly(ethylene oxide) (PEO_{114}-NC, 3 equiv.) to yield PS_{190}-*b*-PEO_{114} diblock copolymer ($M_{n,\ SEC\ (THF)}$ = 27.8 kg mol^{-1}, $Đ$ = 1.16). All prepared PS-*b*-PEO diblock copolymers were stored under nitrogen atmosphere at 4 °C prior to orientation to prevent them from any moisture-mediated hydrolysis of the boronate junction.

Instrumentation

End-group functionalized polystyrene and diblock copolymers were analyzed by size exclusion chromatography (SEC) at room temperature using tetrahydrofuran (THF) as the mobile phase at a flow rate of 1 mL min^{-1} and at a polymer concentration of 3 mg mL^{-1} after filtration through a 0.45 μm PTFE membrane. SEC analyses were performed on a system equipped with a Spectra Physics P100 pump, two PL gel 5 μm mixed-C columns from Polymer Laboratories in series and a Shodex RI 71 refractive index detector. The system was calibrated with polystyrene standards from Polymer Source. PEO was analyzed by SEC in aqueous conditions (solvent: 0.5 M $NaNO_3$ + 0.01 M NaH_2PO_4 (pH 2); column: POE AQUEUX $LiNO_3$ NaN_3) after filtration through a 0.45 μm RC membrane. The structures of the synthesized compounds were confirmed by ^{1}H NMR spectroscopy using a Bruker Avance II spectrometer operating at a resonance frequency of 400 and 100 MHz for hydrogen and carbon nuclei, respectively. Samples were dissolved in deuterated chloroform ($CDCl_3$), dimethylsulfoxide (DMSO-d_6) or deuterium oxide (D_2O) as solvents, and the sample concentration was around 10 mg mL^{-1} for ^{1}H NMR and 40 mg mL^{-1} for ^{13}C NMR experiments. ^{1}H and ^{13}C NMR spectra were recorded at 25 °C and chemical shifts were expressed in ppm with respect to tetramethylsilane (TMS). Scanning Electron Microscopy (SEM) observations were performed on a MERLIN microscope from Zeiss equipped with InLens and Secondary Electron

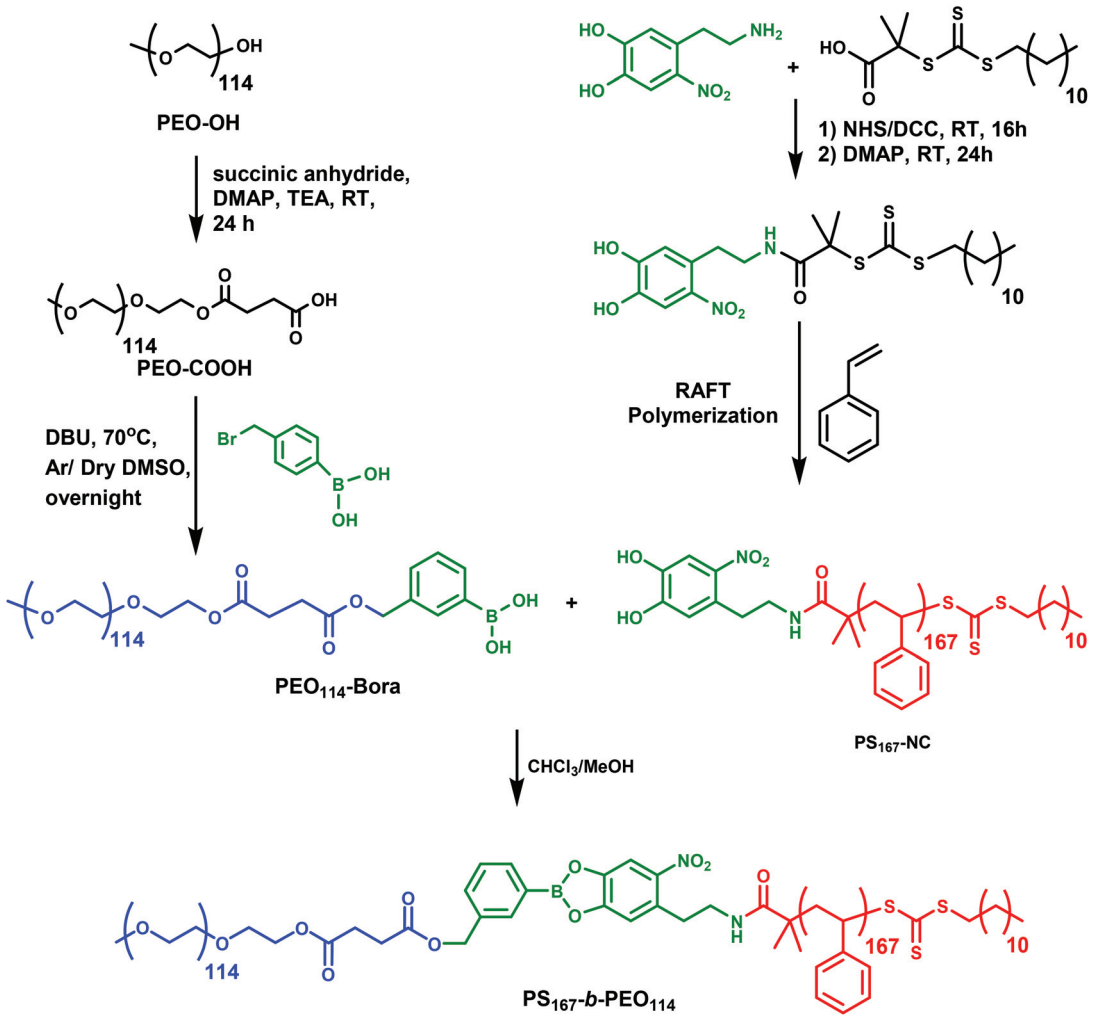

Scheme 1 Synthetic pathway towards boronate linked PS-*b*-PEO diblock copolymers by coupling reaction between nitrocatechol-ended PS and boronic acid-functionalized PEO homopolymers.

detectors using low accelerating voltage (3 kV). Prior to analyses, the samples were coated with a 2 nm layer of platinum in a Cressington 208 HR sputter-coater. Energy-dispersive X-ray spectroscopy (EDX) analyses were performed using an SSD X-Max detector of 50 mm^2 from Oxford Instruments (127 eV for the Kα of Mn). UV-Vis spectra were recorded in UV quartz (1 mm length × 10 mm width × 45 mm height) cuvettes between 200 and 600 nm on a Cary 60 UV-Vis Spectrophotometer from Agilent Technologies, using 1 wt% polymer solution in toluene.

Results and discussion

Synthesis of PS-*b*-PEO diblock copolymers by coupling of corresponding homopolymers

First, boronic acid end-functionalized PEO (MeO-PEO-Bora) was synthesized by esterification of carboxylated PEO (MeO-PEO-COOH) with 3-(bromomethyl)phenylboronic acid. Nitrocatechol end-functionalized PEO (MeO-PEO-NC) was obtained through amidation of MeO-PEO-COOH. The carboxylation of MeO-PEO-OH was conveniently attained through esterification using an excess of succinic anhydride (SAH) in the presence of a nucleophilic catalyst at room temperature. The pure product was obtained after dialysis of the as-product, as demonstrated by ^{1}H NMR spectrometry (Fig. 1b and Fig. S1, ESI†). Boronic acid end-functionalized PEO (MeO-PEO-Bora) was prepared in 73% yield while nitrocatechol end-functionalized PEO (MeO-PEO-NC) was obtained in 87% yield after purification. The chemical structures and end-group functionality were analyzed from the representative ^{1}H NMR (Fig. 1c). The resonance signals from the methyl (δ = 3.38 ppm), methylene (δ = 3.51 ppm), and hydroxyl (δ = 4.58 ppm) groups characteristic of the PEO homopolymer (Fig. 1a) were observed. Fig. 1b displaying the ^{1}H NMR spectrum of carboxylated PEO showed the disappearance of the resonance signal of hydroxyl proton together with the appearance of resonance signals at 4.11 ppm (s, 2H) and 2.56 ppm (s, 4H) ascribed to methylene protons

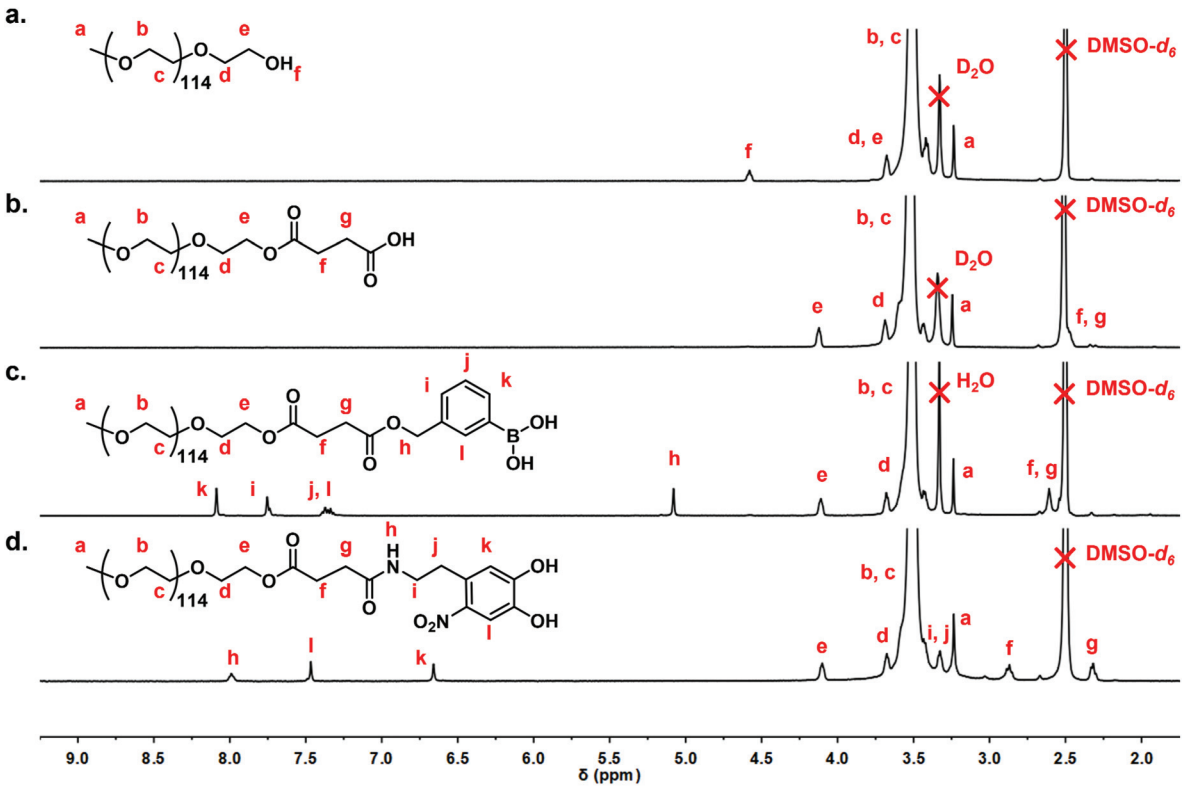

Fig. 1 ^{1}H NMR spectra of: (a) MeO-PEO$_{114}$-OH in D_2O, (b) carboxylic acid end-functionalized PEO$_{114}$ (MeO-PEO$_{114}$-COOH) in D_2O, (c) boronic acid end-functionalized PEO$_{114}$ (MeO-PEO$_{114}$-Bora) in DMSO-d_6 and (d) nitrocatechol end-functionalized PEO$_{114}$ (MeO-PEO$_{114}$-NC) in DMSO-d_6.

arising from SAH, thus confirming the successful carboxylation of PEO. As clearly observed on the ^{1}H NMR spectrum of MeO-PEO-Bora (Fig. 1c), the appearance of resonance signals at 5.1 ppm (s, –CH_2–), 8.09 ppm (s, Ar–CH–) and 7.76 ppm (s, Ar–CH–) indicated the successful functionalization of MeO-PEO-COOH with boronic acid. The reaction of MeO-PEO-COOH with nitrodopamine (ND) yielded MeO-PEO-NC, as confirmed by the appearance of resonance signals characteristic of secondary amide and aromatic protons at 8.00 ppm (s, –NH–), 7.48 ppm (s, Ar–H_2), and 6.67 ppm (d, Ar–H_5) and chemical shift of methylene protons at 3.30–3.36 ppm (m, –CONH–CH_2–CH_2–), 2.89 ppm (d, –CH_2–CH_2–CONH–), and 2.33 ppm (d, –CH_2–CONH–) (Fig. 1d). The chain end functionality of MeO-PEO-Bora and MeO-PEO-NC were determined from the ^{1}H NMR spectroscopic analyses (by comparing the resonance integrals of aromatic –CH– against terminal –OCH_3 (δ = 3.3 (s)) to be as high as 91% and 94%, respectively, as shown on Fig. S6 and S7 in the ESI.† The M_n values of MeO-PEO-Bora and MeO-PEO-NC were consistent with the initial molar mass of MeO-PEO-OH, indicating the successful modification of PEO end-functionality without altering the PEO polymeric backbone.

Nitrocatechol and boronic acid end-functionalized polystyrene (PS-NC and PS-Bora) homopolymers were obtained by RAFT polymerization of styrene using DDMAT-NC or CTA-Bora, respectively. ^{1}H and ^{13}C NMR with COSY and HSQC analyses (Fig. S8–S11, ESI†) confirmed the successful functionalization of DDMAT RAFT agent by catechol functional group using nitro-dopamine hemisulfate. DDMAT-NC and CTA-Bora were prepared by using a recent literature procedure.[36] ^{1}H and ^{13}C NMR analyses are presented in Fig. S12–S15 (ESI†). The RAFT polymerization of styrene using DDMAT-NC or CTA-Bora was performed in 1,4-dioxane for 48 h with conversion from 39% up to 52%, as observed by ^{1}H NMR (Fig. S12 and S13, ESI†). It yielded catechol and boronic acid end-functionalized polystyrenes with narrow molar mass distributions, *i.e.* dispersity indexes $Đ$ = 1.15 and 1.08, respectively (Fig. 3). The chemical structures and M_n values of PS-NC and PS-Bora were determined by ^{1}H NMR (Fig. 2, Fig. S12 and S13, ESI†).

As depicted in Scheme 1, the preparation of PS-*b*-PEO diblock copolymers containing a boronate ester junction was conducted using the coupling reaction between boronic acid and nitrocatechol end-functionalized poly(ethylene oxide) (MeO-PEO-Bora) and polystyrene (PS-NC), respectively. The coupling between functionalized PEO and PS was performed in a nonpolar hydrophobic solvent in the presence of MeOH ($CHCl_3$/MeOH, 20 : 1) under reflux. The reaction was favourably directed toward the formation of boronate ester linkage by constantly removing water by-product using a Dean Stark apparatus equipped with a drying agent, *i.e.* molecular sieves. The addition of MeOH was intended to inhibit the formation of boroxine anhydride and thus to promote the formation of boronate ester. MeO-PEO-Bora was used in excess to ensure complete coupling of PS-NC.[36,37] The unreacted MeO-PEO$_{114}$-

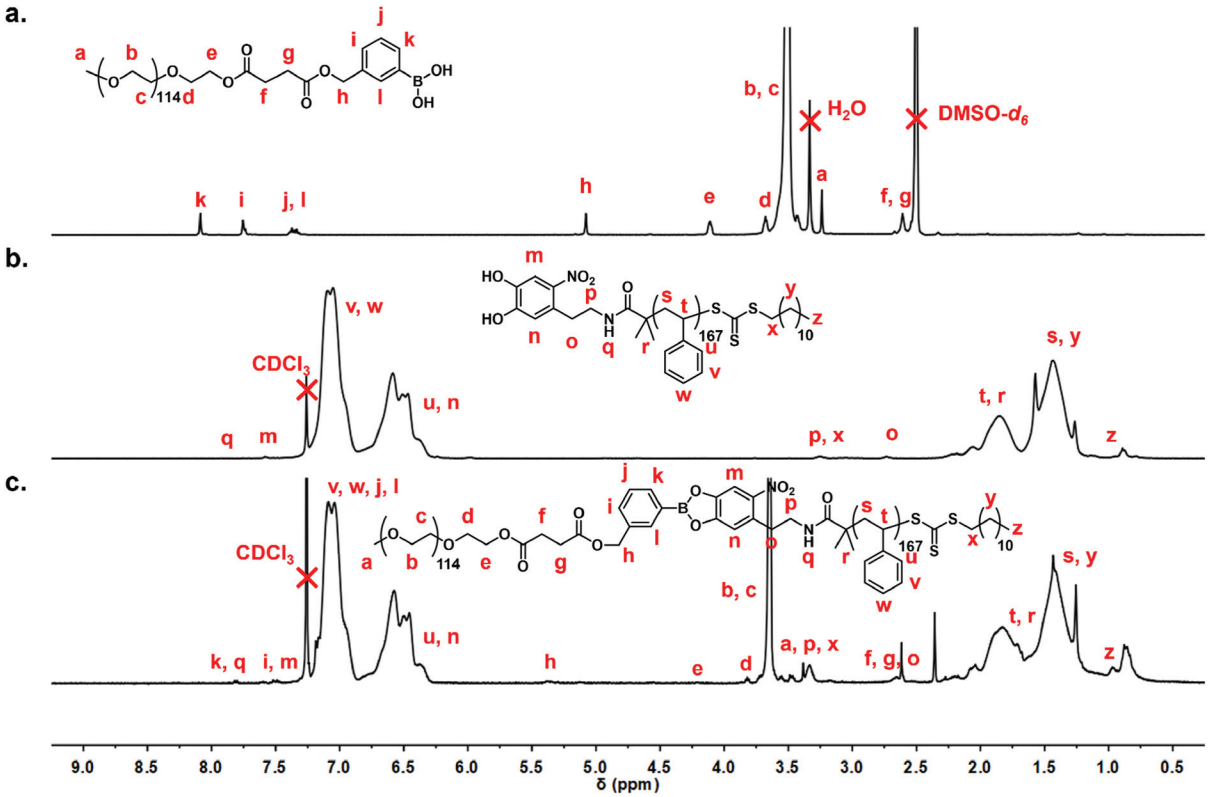

Fig. 2 ^{1}H NMR spectra of (a) boronic acid end-functionalized poly(ethylene oxide) MeO-PEO$_{114}$-Bora in DMSO-d_6, (b) nitrocatechol end-functionalized polystyrene PS$_{167}$-NC in $CDCl_3$ and (c) corresponding block copolymer PS$_{167}$-*b*-PEO$_{114}$ in $CDCl_3$.

Bora was readily removed from the crude product *via* precipitation in cold dry toluene followed by filtration using a PTFE filter adapted on a syringe. The coupling of PEO$_{114}$-Bora and PS$_{167}$-NC afforded a well-defined PS$_{167}$-*b*-PEO$_{114}$ block copolymer with $M_{n\ (SEC,\ THF)}$ = 23.6 kg mol^{-1} and $Đ$ = 1.24 (Fig. 3), as demonstrated by a single peak with a clear shift toward lower retention times than those of corresponding homopolymers. Furthermore, the ^{1}H NMR spectroscopy analysis displayed the characteristic chemical shifts of both PS and PEO blocks (Fig. 2). ^{1}H NMR spectrum of PS$_{167}$-*b*-PEO$_{114}$ revealed characteristic resonance signals of both polystyrene (6.97 ppm (Ar–H), 6.5 (Ar–H), 1.76 ppm (Ar–CH–), 1.36 ppm (–CH_2–)) and PEO (3.7–3.5 (–CH_2–CH_2–O–) blocks. The respective block ratios of PS$_{167}$-*b*-PEO$_{114}$ calculated from ^{1}H NMR spectrum were consistent with the estimated theoretical values from the M_n values of coupled homopolymers. Likewise, PEO$_{114}$-NC and PS$_{190}$-Bora were coupled to obtain PS$_{190}$-*b*-PEO$_{114}$ whose ^{1}H NMR spectrum is presented in Fig. S15.† Hence, the PEO domain volume fractions were calculated as $f_{PEO} = V_{PEO}/(V_{PEO} + V_{PS})$ using bulk densities (1.05 and 1.08 g cm^{-3} for PS and PEO, respectively). The synthesized block copolymers contained PEO block of volume fraction (f_{PEO}) equal to 0.24 and 0.20 which should theoretically develop a morphology of hexagonally close-packed PEO cylinders in a PS matrix. The molecular characteristics of the synthesized homopolymers and corresponding diblock copolymers are summarized in Table 1.

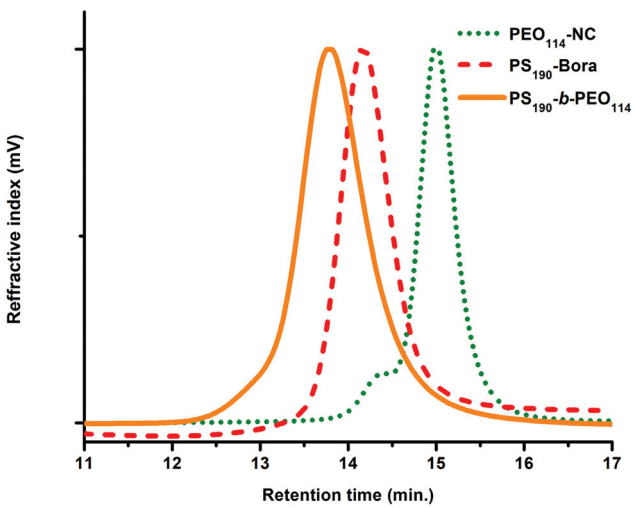

Fig. 3 SEC traces of MeO-PEO$_{114}$-NC, PS$_{190}$-Bora and corresponding diblock copolymer PS$_{190}$-*b*-PEO$_{114}$ in THF as the eluent.

Generation of nanoporous thin films

PS-*b*-PEO thin films were prepared by spin-coating a solution of diblock copolymer in toluene (0.7 wt%) on a silicon wafer. Subsequently, the as-cast films were subjected to solvent vapor annealing in a toluene/water vapor environment controlled at 50 °C to orient the cylindrical PEO microdomains orthogonally

Table 1 Molecular features of synthesized (co)polymers

Sample name	Conversion % (^{1}H NMR)	$M_{n,\,theor}$ (kg mol^{-1})	$M_{n,\,NMR}$ [c] (kg mol^{-1})	$M_{n,\,SEC}$ [d] (kg mol^{-1})	$Đ$	f_{PEO} [e]
PS_{167}-NC	39	16.8[a]	17.3	18.3	1.15	—
PEO_{114}-Bora	—	5.5	5.4	5.9	1.05	—
PS_{167}-*b*-PEO_{114}	—	22.9[b]	23.8	23.6	1.24	0.24
PS_{190}-Bora	52	21.9[a]	19.7	21.3	1.08	—
PEO_{114}-NC	—	5.6	5.7	5.5	1.07	—
PS_{190}-*b*-PEO_{114}	—	25.1[b]	28.0	27.8	1.16	0.2

[a] $M_{n,\,theor,\,PS} = M_{CTA} + conv. \times ([Sty]_0/[CTA]_0) \times M_{styrene}$. [b] $M_{n,\,theor,\,PS\text{-}b\text{-}PEO} = M_n$ (PS) + M_n (PEO). [c] $M_{n,\,NMR}$: number-average molar mass as determined by ^{1}H NMR. [d] SEC measurements with polystyrene standards using THF as eluent. [e] f_{PEO} (volume fraction of PEO block) calculated from M_n, NMR [$f = V_{PEO}/(V_{PEO} + V_{PS})$], the densities of PS and PEO are 1.05 and 1.08, respectively.

to the film surface, as already reported in the literature.[39] As hypothesized, the generation of nanoporous structures requires the selective cleavage of the boronate ester junction to remove the cylindrical domains, *i.e.* PEO segments, and thus generate the oriented nanoporosity. It is well documented that boronate ester can readily split into its two constituents (*i.e.* boronic acid and 1,2 or 1,3-diol groups) *via* hydrolysis or exchange of the involved diol with another one. The acid cleavage of PS_{167}-*b*-PEO_{114} and PS_{190}-*b*-PEO_{114} diblock copolymers was investigated by UV-vis spectroscopy (Fig. 4) and SEC (Fig. S17, ESI†). The absorbance band at 360–430 nm disappeared upon addition of TFA solution. In parallel, SEC analysis of the PS_{190}-*b*-PEO_{114} diblock copolymer after TFA treatment displayed a polymodal distribution consisting of two main peaks corresponding to PEO_{114}-NC and PS_{190}-Bora but also to a less intense peak attributed to the corresponding diblock copolymer that either has not been totally hydrolyzed or spontaneously forms in solvent. In bulk, different conditions related to the steric effect should be considered to break the boronate chemical junction and gently remove the sacrificial block from the nanostructured film. First, the stimuli must be very efficient to break the targeted junction, while remaining chemically inert towards substrate and main polymer matrix. The stimuli must also suitably penetrate the depth of the film while maintaining the dimensional integrity of the film and the fidelity of the end-group functionalities. For our system, the hydrolysis in aqueous medium proved to be inefficient due to the strongly hydrophobic nature of the polystyrene matrix, which restricted water to access the boronate ester junctions easily. The addition of acid in aqueous medium was ineffective in removing the sacrificial block. To overcome this steric hindrance, ethanol was used to facilitate the penetration of acid in the hydrophobic polystyrene matrix. To generate nanopores, nanostructured films were therefore immersed in ethanol solution containing 1 wt% trifluoroacetic acid to split boronate ester junction, while extracting the PEO block in ethanol selectively.

SEM images of PS_{167}-*b*-PEO_{114} thin films are displayed in Fig. 5a & b. The thin film that was immersed in ethanol showed a partial pore opening which indicated a slight removal of PEO domains (Fig. 5a). After treatment in acidic conditions (trifluoroacetic acid solution in EtOH), the formation of ordered cylindrical pores orientated orthogonally to the silicon surface could be clearly observed, as highlighted in

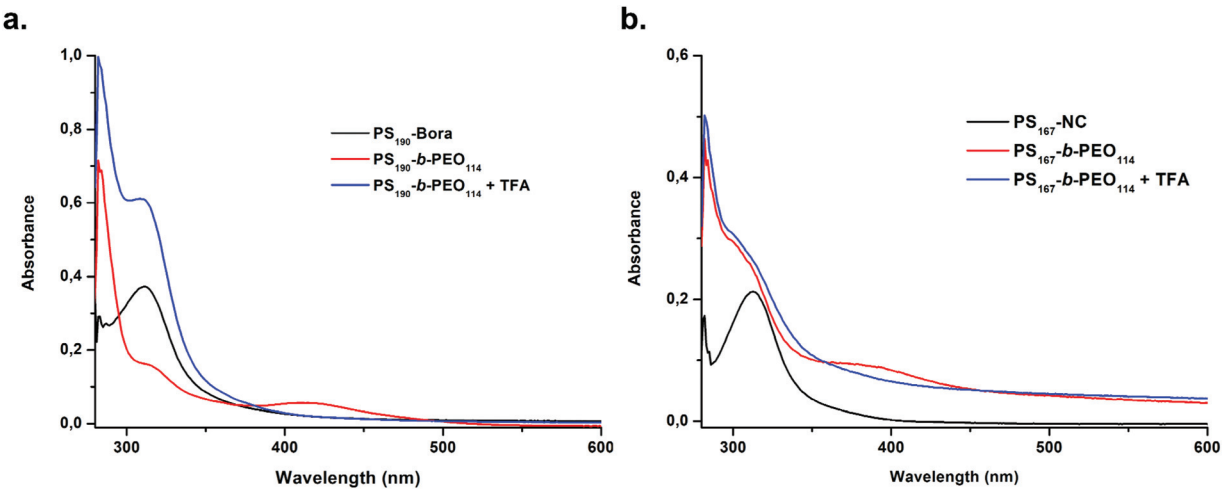

Fig. 4 (a). UV-vis spectra of PS_{190}-Bora (black trace), resulting PS_{190}-*b*-PEO_{114} diblock copolymer (red trace) and same diblock copolymer in a TFA solution in toluene (blue trace). (b). UV-vis spectra of PS_{167}-NC (black trace), resulting PS_{167}-*b*-PEO_{114} diblock copolymer (red trace) and same diblock copolymer in a TFA solution in toluene (blue trace).

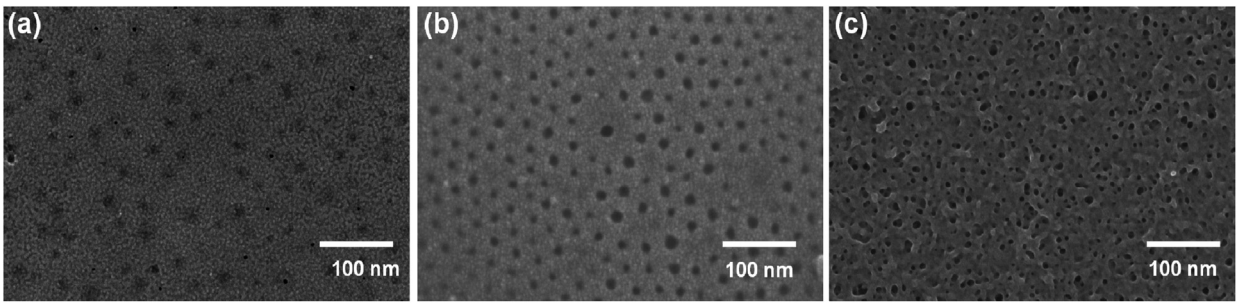

Fig. 5 SEM micrographs of nanoporous polymeric material obtained from (a) PS_{167}-*b*-PEO_{114} treated in ethanol, (b) PS_{167}-*b*-PEO_{114} immersed in a TFA ethanol solution and (c) PS_{190}-*b*-PEO_{114} treated in a TFA ethanol solution.

Fig. 5b. This demonstrated acid-catalyzed hydrolysis's efficiency in breaking the boronate ester junction under mild conditions. An average center-to-center distance between adjacent pores was determined to be approximately 38 nm with an average pore diameter of 12 nm (Fig. 5b). These dimensions were consistent with those obtained from previous nanoporous polystyrene films prepared from PS-*b*-PEO block copolymer reported elsewhere and having similar molecular features.[21,22,25,40,41] For PS_{190}-*b*-PEO_{114} thin films, a nanoporous structure was observed (Fig. 5c), but with smaller nanopores (*i.e.* average pore diameter is around 7 nm) disorganized within the PS matrix. When considering the χN value of PS_{190}-*b*-PEO_{114}, the obtained disorganized nanoporous structure could be explained by the low volume fraction of PEO block, *i.e.* f_{PEO} = 0.20. These results demonstrated that a mild acidic solution is efficient to selectively cleave the boronate ester chemical junction to generate nanoporous thin films containing reactive functional groups at the interface, *e.g.* boronic acid or catechol moieties.

The selective removal of PEO block was evidenced by ^{1}H NMR spectroscopy (Fig. S16, ESI†). After extraction of PEO block in ethanol in acidic solution, the resulting thin film was dissolved in $CDCl_3$ and subsequently analyzed by ^{1}H NMR. As shown in Fig. S16,† as expected, the nanoporous thin film is mainly characterized by proton resonance signals corresponding to the polystyrene block. The observed proton resonance signal at 3.5 ppm was attributed to the traces of PEO blocks trapped in the oxide layer of the substrate. It was found out that 3.5% of the initial amount ot PEO remain in the oxide layer, as calculated by comparison of the integral of the PEO proton signals with those of the PS-*b*-PEO precursor diblock copolymer.

Conclusions

We have successfully synthesized a cleavable PS-*b*-PEO block copolymer *via* a coupling reaction between corresponding catechol and boronic acid-ended homopolymers under mild experimental conditions. The key step in the copolymer design was to incorporate a reversible boronate ester junction between polystyrene and poly(ethylene oxide) blocks. Generation of nanoporous material was achieved through self-assembly of block copolymer, orientation of phase separated domains using solvent annealing and selective removal of sacrificial block. Molecular structures were confirmed by ^{1}H NMR and SEC, while morphological characteristics were analyzed by SEM. Hence, we demonstrated the potential of using a boronate ester as a cleavable junction to prepare functional nanoporous materials. The facile cleavage of boronate ester was performed under mild acidic environment. The obtained functionalized nanopores featured surfaces decorated either by catechol or boronic acid groups, which could be readily exploited due to their versatile reactivity to tune the surface chemistry for specific applications. In particular, our investigations regarding the use of these functionalized nanoporous materials as sustainable and recyclable supports for enzyme immobilization, protein separation or heterogeneous catalysis will be reported in due course.

Conflicts of interest

There are no conflicts to declare.

Acknowledgements

The authors acknowledge financial support from CNRS through Emergence@INC 2019 project. DF and PW would like to thank the Chevreul Institute for its help in the development of this work through the ARCHI-CM project supported by the "Ministère de l'Enseignement Supérieur de la Recherche et de l'Innovation", the region "Hauts-de-France", the ERDF program of the European Union and the "Métropole Européenne de Lille".

References

1 K. V. Peinemann, V. Abetz and P. F. W. Simon, Asymmetric superstructure formed in a block copolymer via phase separation, *Nat. Mater.*, 2007, **6**, 992–996.

2 M. W. Matsen and F. S. Bates, Unifying Weak- and Strong-Segregation Block Copolymer Theories, *Macromolecules*, 1996, **29**, 1091–1098.
3 F. S. Bates and G. H. Fredrickson, Block Copolymer Thermodynamics: Theory and Experiment, *Annu. Rev. Phys. Chem.*, 1990, **41**, 525–557.
4 D. A. Olson, L. Chen and M. A. Hillmyer, Templating Nanoporous Polymers with Ordered Block Copolymers, *Chem. Mater.*, 2008, **20**, 869–890.
5 E. A. Jackson and M. A. Hillmyer, Nanoporous Membranes Derived from Block Copolymers: From Drug Delivery to Water Filtration, *ACS Nano*, 2010, **4**, 3548–3553.
6 A. S. Zalusky, R. Olayo-Valles, J. H. Wolf and M. A. Hillmyer, Ordered Nanoporous Polymers from Polystyrene–Polylactide Block Copolymers, *J. Am. Chem. Soc.*, 2002, **124**, 12761–12773.
7 A. S. Zalusky, R. Olayo-Valles, C. J. Taylor and M. A. Hillmyer, Mesoporous Polystyrene Monoliths, *J. Am. Chem. Soc.*, 2001, **123**, 1519–1520.
8 S. Y. Yang, I. Ryu, H. Y. Kim, J. K. Kim, S. K. Jang and T. P. Russell, Nanoporous Membranes with Ultrahigh Selectivity and Flux for the Filtration of Viruses, *Adv. Mater.*, 2006, **18**, 709–712.
9 H. Uehara, T. Yoshida, M. Kakiage, T. Yamanobe, T. Komoto, K. Nomura, K. Nakajima and M. Matsuda, Nanoporous Polyethylene Film Prepared from Bicontinuous Crystalline/Amorphous Structure of Block Copolymer Precursor, *Macromolecules*, 2006, **39**, 3971–3974.
10 T. Thurn-Albrecht, R. Steiner, J. DeRouchey, C. M. Stafford, E. Huang, M. Bal, M. Tuominen, C. J. Hawker and T. P. Russell, Nanoscopic Templates from Oriented Block Copolymer Films, *Adv. Mater.*, 2000, **12**, 787–791.
11 J. Rzayev and M. A. Hillmyer, Nanochannel Array Plastics with Tailored Surface Chemistry, *J. Am. Chem. Soc.*, 2005, **127**, 13373–13379.
12 L. M. Pitet, M. A. Amendt and M. A. Hillmyer, Nanoporous Linear Polyethylene from a Block Polymer Precursor, *J. Am. Chem. Soc.*, 2010, **132**, 8230–8231.
13 H. Mao and M. A. Hillmyer, Nanoporous Polystyrene by Chemical Etching of Poly(ethylene oxide) from Ordered Block Copolymers, *Macromolecules*, 2005, **38**, 4038–4039.
14 M. Zhang, L. Yang, S. Yurt, M. J. Misner, J.-T. Chen, E. B. Coughlin, D. Venkataraman and T. P. Russell, Highly Ordered Nanoporous Thin Films from Cleavable Polystyrene-block-poly(ethylene oxide), *Adv. Mater.*, 2007, **19**, 1571–1576.
15 S. Yurt, U. K. Anyanwu, J. R. Scheintaub, E. B. Coughlin and D. Venkataraman, Scission of Diblock Copolymers into Their Constituent Blocks, *Macromolecules*, 2006, **39**, 1670–1672.
16 J. T. Goldbach, T. P. Russell and J. Penelle, Synthesis and Thin Film Characterization of Poly(styrene-block-methyl methacrylate) Containing an Anthracene Dimer Photocleavable Junction Point, *Macromolecules*, 2002, **35**, 4271–4276.
17 J. T. Goldbach, K. A. Lavery, J. Penelle and T. P. Russell, Nano- to Macro-Sized Heterogeneities Using Cleavable Diblock Copolymers, *Macromolecules*, 2004, **37**, 9639–9645.
18 C.-A. Fustin, B. G. G. Lohmeijer, A.-S. Duwez, A. M. Jonas, U. S. Schubert and J.-F. Gohy, Nanoporous Thin Films from Self-Assembled Metallo- Supramolecular Block Copolymers, *Adv. Mater.*, 2005, **17**, 1162–1165.
19 K. Satoh, J. E. Poelma, L. M. Campos, B. Stahl and C. J. Hawker, A facile synthesis of clickable and acid-cleavable PEO for acid-degradable block copolymers, *Polym. Chem.*, 2012, **3**, 1890–1898.
20 R. Poupart, A. Benlahoues, B. Le Droumaguet and D. Grande, Porous Gold Nanoparticle-Decorated Nanoreactors Prepared from Smartly Designed Functional Polystyrene-block-Poly(d,l-Lactide) Diblock Copolymers: Toward Efficient Systems for Catalytic Cascade Reaction Processes, *ACS Appl. Mater. Interfaces*, 2017, **9**, 31279–31290.
21 H. Zhao, W. Gu, E. Sterner, T. P. Russell, E. B. Coughlin and P. Theato, Highly Ordered Nanoporous Thin Films from Photocleavable Block Copolymers, *Macromolecules*, 2011, **44**, 6433–6440.
22 J.-M. Schumers, A. Vlad, I. Huynen, J.-F. Gohy and C.-A. Fustin, Functionalized Nanoporous Thin Films From Photocleavable Block Copolymers, *Macromol. Rapid Commun.*, 2012, **33**, 199–205.
23 J.-M. Schumers, J.-F. Gohy and C.-A. Fustin, A versatile strategy for the synthesis of block copolymers bearing a photocleavable junction, *Polym. Chem.*, 2010, **1**, 161–163.
24 M. Kang and B. Moon, Synthesis of Photocleavable Poly (styrene-block-ethylene oxide) and Its Self-Assembly into Nanoporous Thin Films, *Macromolecules*, 2009, **42**, 455–458.
25 C. G. Gamys, J.-M. Schumers, A. Vlad, C.-A. Fustin and J.-F. Gohy, Amine-functionalized nanoporous thin films from a poly(ethylene oxide)-block-polystyrene diblock copolymer bearing a photocleavable o-nitrobenzyl carbamate junction, *Soft Matter*, 2012, **8**, 4486–4493.
26 C. G. Gamys, J.-M. Schumers, C. Mugemana, C.-A. Fustin and J.-F. Gohy, Pore-Functionalized Nanoporous Materials Derived from Block Copolymers, *Macromol. Rapid Commun.*, 2013, **34**, 962–982.
27 H. Yu, F. Stoffelbach, C. Detrembleur, C.-A. Fustin and J.-F. Gohy, Nanoporous thin films from ionically connected diblock copolymers, *Eur. Polym. J.*, 2012, **48**, 940–944.
28 J.-H. Ryu, S. Park, B. Kim, A. Klaikherd, T. P. Russell and S. Thayumanavan, Highly Ordered Gold Nanotubes Using Thiols at a Cleavable Block Copolymer Interface, *J. Am. Chem. Soc.*, 2009, **131**, 9870–9871.
29 B. Le Droumaguet, R. Poupart and D. Grande, "Clickable" thiol-functionalized nanoporous polymers: from their synthesis to further adsorption of gold nanoparticles and subsequent use as efficient catalytic supports, *Polym. Chem.*, 2015, **6**, 8105–8111.
30 J. Rao, S. De and A. Khan, Synthesis and self-assembly of dynamic covalent block copolymers: towards a general

route to pore-functionalized membranes, *Chem. Commun.*, 2012, **48**, 3427–3429.

31 M. Glassner, J. P. Blinco and C. Barner-Kowollik, Formation of nanoporous materials via mild retro-Diels–Alder chemistry, *Polym. Chem.*, 2011, **2**, 83–87.

32 U. Mansfeld, C. Pietsch, R. Hoogenboom, C. R. Becer and U. S. Schubert, Clickable initiators, monomers and polymers in controlled radical polymerizations – a prospective combination in polymer science, *Polym. Chem.*, 2010, **1**, 1560–1598.

33 S. K. Varshney, J.-X. Zhang, J. Ahmed, Z. Song, V. Klep and I. Luzinov, Synthesis of poly(styrene-block-ethylene oxide) copolymers by anionic polymerization and acid cleavage into its constituent homopolymers for the formation of ordered nanoporous thin films, *e-Polymers*, 2008, **8**, 094.

34 W. H. Binder and R. Sachsenhofer, 'Click' Chemistry in Polymer and Material Science: An Update, *Macromol. Rapid Commun.*, 2008, **29**, 952–981.

35 C. E. Hoyle and C. N. Bowman, Thiol–Ene Click Chemistry, *Angew. Chem., Int. Ed.*, 2010, **49**, 1540–1573.

36 F. Coumes, A. Malfait, M. Bria, J. Lyskawa, P. Woisel and D. Fournier, Catechol/boronic acid chemistry for the creation of block copolymers with a multi-stimuli responsive junction, *Polym. Chem.*, 2016, **7**, 4682–4692.

37 F. Coumes, P. Woisel and D. Fournier, Facile Access to Multistimuli-Responsive Self-Assembled Block Copolymers via a Catechol/Boronic Acid Ligation, *Macromolecules*, 2016, **49**, 8925–8932.

38 M. Rodenstein, S. Zürcher, S. G. P. Tosatti and N. D. Spencer, Fabricating Chemical Gradients on Oxide Surfaces by Means of Fluorinated, Catechol-Based, Self-Assembled Monolayers, *Langmuir*, 2010, **26**, 16211–16220.

39 T. Ghoshal, J. O'Connell, C. Sinturel, P. Andreazza, J. D. Holmes and M. A. Morris, Solvent mediated inclusion of metal oxide into block copolymer nanopatterns: Mechanism of oxide formation under UV-Ozone treatment, *Polymer*, 2019, **173**, 197–204.

40 C. Sinturel, F. S. Bates and M. A. Hillmyer, High χ–Low N Block Polymers: How Far Can We Go?, *ACS Macro Lett.*, 2015, **4**, 1044–1050.

41 Y. Zhang, R. A. Mulvenna, S. Qu, B. W. Boudouris and W. A. Phillip, Block Polymer Membranes Functionalized with Nanoconfined Polyelectrolyte Brushes Achieve Sub-Nanometer Selectivity, *ACS Macro Lett.*, 2017, **6**, 726–732.